Supplementary Information for

Early gigantic lamniform marks the onset of mega-body size in modern shark evolution

Mohamad Bazzi[1,*], Mikael Siversson[2,3], Sabine Wintner[4,5], Michael Newbrey[6], Jonathan L. Payne[1], Nicolás E. Campione[7], Aubrey J. Roberts[8], Lisa J. Natanson[9], Stephen Hall[10], Tatianna Blake[11], and Benjamin P. Kear[12]

[1]Department of Earth and Planetary Sciences, Stanford University, Stanford, CA 94305, USA.
[2]Western Australian Museum, Collections and Research Centre, 49 Kew Street, Welshpool, WA 6106, Australia.
[3]School of Molecular and Life Sciences, Curtin University, Bentley, WA 6102, Australia.
[4]KwaZulu-Natal Sharks Board, Private Bag 2, Umhlanga Rocks, 4320, South Africa.
[5]School of Life Sciences, University of KwaZulu-Natal, Durban, 4000, South Africa.
[6]Department of Biology, Columbus State University, Columbus, GA, USA.
[7]Palaeoscience Research Centre, School of Environmental and Rural Science, University of New England, Armidale, NSW 2351, Australia.
[8]Natural History Museum, University of Oslo, P.O. Box 1172 Blindern, NO-0318 Oslo, Norway.
[9]Retired NOAA/NMFS, Narragansett Laboratory 28 Tarzwell Dr. Narragansett, RI 02882, USA.
[10]Division of Solid Mechanics, Lund University, Ole Römers väg 1, SE-223 63 Lund, Sweden.
[11]Killeen Independent School District, 200 N W S Young Dr. Killeen, TX 76543-4025, USA.
[12]Department of Palaeobiology, Swedish Museum of Natural History, SE-104 05 Stockholm, Sweden.

*Corresponding author. Email: bazzi@stanford.edu

Institutional abbreviations

AMNH, American Museum of Natural History New York, U.S.A. FHSM, Sternberg Museum of Natural History, Hays, U.S.A. KUVP, University of Kansas Museum of Natural History, Lawrence, U.S.A. LACM, Natural History Museum of Los Angeles County, California, U.S.A. LU, Lund University, Lund, Sweden. NHMUK, The Natural History Museum, London, U.K. NHM-UO, Natural History Museum, University of Oslo, Norway. NTM, Museum and Art Gallery of the Northern Territory, Darwin, Australia. OMNH, Sam Noble Oklahoma Museum of Natural History, Norman, U.S.A. SDSM, South Dakota School of Mines and Technology, Rapid City, U.S.A. UALVP, University of Alberta, Laboratory for Vertebrate Paleontology, Edmonton, Canada. UMMZ, University of Michigan, Museum of Zoology, Ann Arbor, U.S.A. USNM, National Museum of Natural History, Smithsonian Institution, Washington, D.C., U.S.A. UWGM, University of Wisconsin, Geology Museum, Madison, U.S.A. WAM, Western Australian Museum, Perth, Australia.

Geological setting

In addition to NTM P 922-33, NTM P 922-32, NTM P 9382, NTM P 922-37, and NTM P 922-29 (Supplementary Figs. 1-2), several other large shark vertebrae have been recovered from the Darwin Formation[1,2], but these have never been described in detail. All the specimens derive from the same shoreline exposures of the Darwin Formation at Casuarina Beach in the northern suburbs of Darwin, Northern Territory, Australia. Lithologically, the Darwin Formation comprises mainly glauconitic sandstone and radiolarian mudstone with a basal quartzose conglomerate and localised nodular phosphorite horizon that marks the uppermost boundary of the unit[3]. The Darwin Formation forms part of the upper Aptian to mid-Turonian Bathurst Island Group succession that rests non-conformably upon Proterozoic basement rocks within the Money Shoals Platform[3]. The Darwin Formation was laid down under inner-shelf conditions along the eastern Gondwanan margin of the southern Tethys palaeo-ocean[3,4]. The rarity of benthic invertebrates suggests a basally anoxic stratified water column[3]. The age-diagnostic belemnite *Peratobelus*[5,6], together with palynomorphs and dinoflagellates are reportedly consistent with the *Diconodinium davidii* zone[3], correlating with a late Aptian age-range[7]. This concurs with the occurrence of leptocleidid plesiosaurians[8], which are a widespread group throughout Aptian marine units in Australia[9,10].

X-ray microtomography

X-ray microtomography data was acquired for NTM P922-33 and NTM P922-37 at the LU 4D Imaging Lab using an RX Solutions EasyTom150. The X-ray source settings were 150 kV and 500 mA with a 20 mm spot size. Two filters were placed in front of the source to reduce beam hardening effects: 0.35 mm copper and 0.3 mm steel. The sample was placed at 187.82 mm and the detector at 611.65 mm from the source giving an effective pixel size of 39 µm. To fit the full sample width in the field of view two overlapping projections were acquired at each angle and 2880 projection images were acquired over 360° sample rotation. Even with the source filters beam hardening was observed in the reconstructed images so a beam hardening correction was applied during the reconstruction. The tomographic reconstruction was performed using the RX solutions Xact software to give the final image volumes with cubic voxels of width 39 µm.

Microtomographic image rendering

Microtomographic image rendering was undertaken at NHM-UO. Two scans of NTM P922-33 and NTM P922-37 were merged to form single high-resolution images and down sampled to 8bit unsigned in Avizo (v.2020.2). Tomographic acquisition was performed under step rotation with 3,016 projections over 360°. For the most complete centrum (NTM P922-33), scans had a voxel size of 0.0753767 mm^3. A 0.5 mm tin filter was utilised. The beam energy set to 180 keV, 230 uA. Scans visualised in Avizo (v.2020.2) using the orthoslice and volume rendering functions, and scalebars were created for the orthoslices utilising the measurement tool. Images were then exported from slice number 911, halfway through the centrum to measure between the annuli.

Description of the fossils

Comparative specimens

Cardabiodon ricki: WAM 96.3.175 (centra); WAM 96.4.45 (holotype, teeth and centra); WAM 13.6.1 (tooth); UALVP 49430 (tooth). *Cardabiodon venator*: WAM 04.10.64–100 (teeth); WAM 95.7.28 (tooth). *Cretoxyrhina mantelli*: AMNH FF 7210 (teeth, partial head, centra); FHSM VP-323 (teeth, partial head, centra); FHSM VP-2184 (teeth, centra); FHSM VP-2187 (teeth, partial head, centra); KUVP 55060 (teeth, centra). *Cretoxyrhina agassizensis*: WAM 13.6.2 (tooth); DMNH 746C (centrum). *Cretoxyrhina* sp.: NHMUK OR.25939; NHMUK OR.49015. *Cretalamna hattini*: LACM P-128126 (teeth, partial head, centra). *Squalicorax* spp.: FHSM VP-2213 (teeth, jaws); KUVP 69712 (teeth, partial head, centra); LACM P-135929 (teeth, partial head, centra); SDSM 34975 (teeth, partial head, centra); USNM 425665 (teeth, head, centra); UWGM NS.1509.07 (teeth, centra); UWGM NS.1509.34 (teeth, centra). *Archaeolamna kopingensis*: LACM P-128125 (teeth, jaws, centra). *Hypotodus verticalis*: NHMUK OR.12377 (teeth, cartilage, centrum); NHMUK OR.28763 (teeth, cartilage, centrum); NHMUK OR.38867 (teeth, cartilage, centra). *Carcharias taurus*: LACM I-39336-5; UMMZ 147001. *Odontaspis ferox*: LACM I-39445-1. *Alopias superciliosus*: LACM I-39321-1. *Alopias vulpinus*: LACM I-36864-1; LACM I-38158-1; LACM I-39324-1; LACM I-39325-1; LACM I-39330-1. *Isurus paucus*: LACM I-57284-1; LACM I-57285-1. *Isurus oxyrinchus*: LACM I-39470-2. *Carcharodon carcharias*: LACM I-35875-1; LACM I-38194-1; LACM I-42728-1; LACM I-57280-1; LACM I-57281-1; LACM I-57282-1; LACM I-57283-1; LACM I-42094-1; LACM I-42094-2; LACM I-42100-2. *Lamna ditropis*: LACM I-56781-1. *Lamna nasus*: LACM I-38174-1; UMMZ 60591. *Cetorhinus maximus*: LACM I-35593-1.

Terminology

Description of vertebral centra follows[11] except where: cranio-caudal length is referred to as length; medio-lateral breadth is referred to as width; dorso-ventral height is referred to as height. We also follow[12–16] for morphological and growth-related characteristics.

Diagnosis

NTM P 922-33, NTM P 922-32, NTM P 9382, NTM P 922-37, and NTM P 922-29 are distinguished from most other lamniform centra in possessing the following combination of character states: commonly bifurcating radial lamellae near the rostral and caudal surfaces of corpora calcarea that often do not extend to the distal margin. They are classified with Cardabiodontidae in the following combination of character states: short to medium length, round centrum with a very thick corpus calcareum for its length, a corpus calcareum with a distally flat rim, radial lamellae complete and exhibit straight, angled, and meandering patterns, radial lamellae that occur in low density, few circular or subovate large pores concentrated next to each corpus calcareum, and papillose concentric ridges on the surface of the corpora calcarea. They differ from other cardabiodontids in possessing evenly-spaced clusters of highly branched (distally) lateral radial lamellae adjacent to the corpora calcarea forming multiple triangle patterns in septae and subdivided by gracile lamellae or fusing distally into robust lamellae; no additional large subovate or subrectangular foramina that extend to the focus.

Description

NTM P 922-33, NTM P 922-32, NTM P 9382, NTM P 922-37, and NTM P 922-29 are precaudal mid-trunk centra larger in diameter than those of *Cardabiodon ricki* and *Cretoxyrhina. mantelli* (WAM 96.4.45.128, WAM 96.3.175.1, FHSM VP-2184). One centrum from the holotype of *C. ricki* (WAM 96.4.45.128) exhibits an estimated diameter of 84 mm and length of 30 mm. Based on NTM P922-33, the mid-trunk centra are thus 2.6–2.9 times wider than they are long and have a double-cone (biconcave) calcification with shallowly concave lateral sides. The centra of *C. ricki* exhibit a convex lateral surface[12]. The mid-trunk dorsal foramina for articulation with the neural arch are rectangular with rounded corners and extend about 63% of the anteroposterior distance of the intermedialia (NTM P922-33: Supplementary Fig. 1A-B). Ventral foramina are rectangular with rounded corners and extend 79% of the anteroposterior distance of the intermedialia (NTM P922-32 Supplementary Fig. 1C).

The Darwin Formation cardabiodontid centra are round with height equal to width (NTM P922-33: Supplementary Fig. 1A), as in *C. ricki*. The centra are all short, ranging from 0.35 to 0.39 in ratio of length/width. The centrum length/width ratio of *C. mantelli* ranges from 0.28–0.44, with *Cretalamna hattini* ranging from 0.40–0.42[12]. Centrum length is longer in *C. ricki* (0.3–0.51), *Carcharodon carcharias* (0.51), *Isurus paucus* (0.53-0.54: LACM I-57284-1, LACM I-57285-1), *Carcharias taurus* (0.55), *Cetorhinus maximus* (0.61), and *Isurus oxyrinchus* (0.65)[11,12].

The Darwin Formation cardabiodontid centra are septate with complete straight, meandering, and angled lamellae; many lamellae bifurcate distally and terminate as septae (NTM P922-37: Supplementary Fig. 3A, B). By contrast, the septae of *C. ricki* and *C. carcharias* are complete and straight[11,12]. The radial lamellae originate from the focus and are more robust distally with a thickness of 0.7–1.3 mm. The centra of *C. ricki* exhibit radial lamellae with a thickness of 1.3–1.6 mm (WAM 96.4.45.128); or 1.0–1.2 mm in *C. maximus* with centrum diameter of 98 mm[12]. Radial lamellae bifurcate at the rostral and caudal surfaces of corpora calcarean, sometimes repeatedly along the same radial trajectory. Most of the bifurcating lamellae do not reach the distal margin of the centrum (NTM P922-37: Supplementary Fig. 3C-D). The lateral radial lamellae cluster into evenly-spaced groups of highly branched lamellae adjacent to the rostral and caudal surfaces of corpora calcarean and form multiple prominent triangular shapes in the septae; this is not otherwise evident in *C. ricki*, *C. mantelli*, or *C. hattini. Isurus paucus* possesses some distally incomplete lamellae, but these are not regularly or commonly branched, nor are they clustered into triangular shapes (LACM I-57284-1, LACM I-57285-1). An identical condition has been observed in *Lamna nasus*[16]. The radial lamellae of OMNH 68860 bifurcate distally and exhibit distal fusion, with distally incomplete lamellae and indistinct triangular shapes (see[17]). Condition of the incomplete lamellae cannot be confirmed in KUVP 16343 (see[18]).

The Darwin Formation cardabiodontid lack large subovate or subrectangular foramina that extend to the focus and exhibit a continuous rim except for those for the basidorsal and basiventral cartilages. Large subovate or subrectangular foramina with a continuous rim are present in OMNH 68860[17].

In lateral view, the radial lamellae of the Darwin Formation cardabiodontid are gracile (NTM P922-37: Supplementary Fig. 3A-B). The density of radial lamellae is low and clustered sometimes fusing distally into robust radial lamellae with interseptal spaces 3.6–8.3 times the thickness of the lamellae (NTM P922-37: Supplementary Fig. A-B). *Carcharomodus escheri* also exhibits low density, clustered radial lamellae with interseptal spaces 2.1–4.4 times the thickness of the lamellae[19]. Similarly, *C. ricki* has a low density of robust lamellae with interseptal spaces 2.9–3.8 times the thickness of the lamellae; this is identical to *Carcharias taurus*[11] and *Hypotodus verticalis* (NHMUK OR.12377, NHMUK OR.38867)[12]. *Isurus paucus* possess gracile, straight, branched, and low-density lamellae with interseptal spaces 4.9–5.6 times the thickness of the lamellae (LACM I-57284-1, LACM I-57285-1). *Carcharodon carcharias* has moderate density lamellae with interseptal spaces ranging 1.7–1.9 times their thickness (LACM I-3578-1)[12]. OMNH 68860 has robust, branched, straight and meandering, moderate densely packed radial lamellae with interseptal spaces ranging from 1.6–2.4 times the lamellar thickness[17]. By contrast, radial lamellae are gracile and very densely packed in *Archaeolamna kopingensis* (LACM I-128125)[20] and *C. hattini* (LACM P-128126)[21]. The radial lamellae in *C. mantelli* (FHSM VP-323, FHSM VP-2184, FHSM VP-2187, KUVP 55060, DMNH 746C) are densely packed with interseptal spaces 1–1.5 times the thickness of the lamellae (FHSM VP-2184). The radial lamellae of KUVP 16343 are robust, branched, straight, and densely packed with interseptal spaces 1.3 times the thickness of the lamellae. The radial lamellae of *Rhincodon typus* are complete, numerous, and densely packed; however, the sides of the centrum are deeply concave making the centrum spool-shaped in lateral view (UMMZ 128770, WAM P.29547-001)[22]. The radial lamellae of *R. typus* (UMMZ 128770) are proximodistally compressed unlike the lamellae of all other sharks. Growth of the lamellae occur in discrete layers (UMMZ 128770) as opposed to the continuous growth of lamellae of lamniforms or other orectolobiforms.

The intermedialia region between the corpora calcarea is not solid. Concentric lamellae appear to be present adjacent to the corpora calcarea and in the intermedialia (NTM P922-37: Supplementary Fig. 3A–F). These are evidenced by thin lines extending perpendicular from the radial lamellae; however, they are not preserved as complete concentric rings. *Cretoxyrhina mantelli* also exhibits thin concentric lamellae[23]. Concentric lamellae are present in *Alopias vulpinus* (LACM I-38158-1), and *C. maximus* (LACM I-35593-1). Concentric lamellae are not visible in most *C. carcharias* (LACM I-35875-1, LACM I-42094-1, LACM I-57280-1, LACM I-57281-1, LACM I-57282-1, LACM I-57283-1)[12]. There are no concentric lamellae in the intermedialia of centra of *C. ricki* (WAM 96.3.175.1, WAM 96.4.45.128), *A. kopingensis* (LACM P-128125), *C. hattini* (LACM P-128126)[21], *I. paucus* (LACM I-57284-1, LACM I-57285-1), and *I. oxyrinchus* (LACM I-39470-2)[12]. No concentric lamellae are present in KUVP 16343 contrary to[18].

No diagonal septa are present around the dorsal and ventral foramina, nor are they seen in *C. ricki*, *C. mantelli* or *C. hattini*[12]. The diagonal septa are present in centra of *C. maximus*[12].

The biconcave surface of the corpus calcareum shows numerous concentric ridges with papillose texture interspersed by concentric grooves (NTM P922-29, NTM P9382: Supplementary Figs. 1D, 2C-D). The papilose texture is present on the concentric ridges of KUVP 16343 and OMNH 68860[17]. Newbrey *et al.*[12] also reported papilose texture on the concentric ridges of corpora calcarea of *C. ricki*. No papilose texture is present on the corpora calcarea of *I. paucus* (LACM I-57284-1, LACM I-57285-1), *I. oxyrinchus* (LACM I-39470-2), *C. carcharias* (LACM I-35875-1), *A. vulpinus* (LACM I-38158-1), *C. maximus* (LACM I-35593-1), or *C. mantelli* (FSHM VP-2184, FSHM VP-2187), *C. hattini* (LACM P-128126)[21], or *Squalicorax* spp. (KUVP 55190, SDSM 34975, SDSM 82067; UWGM NS.1509.07, UWGM NS.1509.34).

The corpus calcareum is uniformly thickened towards the distal margin with a distal thickness = 5% of the centrum diameter (NTM P922-33: Supplementary Fig. 3G-H). The corpus calcareum exhibits uniform thickness in the centra of *C. mantelli* at ~7–8% (FSHM VP-2184, FSHM VP-2187)[23], *A. kopingensis* (8%)[20], *Cretalamna hattini* (7%, LACM P-128126)[21], *Squalicorax* spp. (3–5%; KUVP 55190, SDSM 34975, 82067; UWGM NS.1509.07, NS.1509.34), and *C. carcharias* (4–7%; LACM I-35875-1)[11]. The corpus calcareum of *I. paucus* is 5% the thickness of the centrum diameter (LACM I-57284-1, LACM I-57285-1), 9% in the tall and narrow centrum of *I. oxyrinchus* (LACM I-39470-2), and 9% in the tall and narrow centrum of *A. vulpinus* (LACM I-38158-1). The corpus calcareum of KUVP 16343[18] also exhibits a uniform thickness at 6.1 mm distally. By contrast, *C. ricki* exhibits 8–11%, *C. maximus* exhibits 9% (LACM I-35593-1)[12]. However, *C. maximus* has a very thin corpus calcareum, but the distal end of the arm of the corpus calcareum greatly thickens in larger centrum sizes (LACM I-35593-1)[12,24].

The thickness of the corpus calcareum is 21% in NTM P922-37, indicating that they are greatly thickened for their length. *Cardabiodon ricki* exhibits an even thicker corpus calcareum being 28% the length of the mid-trunk centrum (WAM 96.3.175.1, WAM 96.4.45.128), and 22% in *I. oxyrinchus* (LACM I-39470-2). The corpus calcareum is much thinner in anterior and mid-trunk precaudal centra of *C. mantelli* (10–16%; AMNH FF 7210, FHSM VP-233, FHSM VP-2187), *A. kopingensis* (14%; LACM P-128125), *C. hattini* (14%; LACM P-128126)[21], *C. carcharias* (9–14%; LACM I-35875-1)[11], *L. nasus* (22%), and *I. paucus* (9-10%; LACM I-57284-1, LACM I-57285-1)[12].

Pores are large (1-2 mm) and subovate and situated adjacent to the anterior and posterior corpora calcarea on the ventral, dorsal, and lateral sides of NTM P922-32, NTM P922-33, and NTM P 922-37. Similar pores (1–2 mm oval foramina) are situated next to the anterior and posterior corpora calcarea near the dorsal and ventral articular foramina of *C. ricki* and *C. mantelli*[12]. *Archaeolamna kopingensis* exhibits round to elongate, subovate pores adjacent to the anterior and posterior corpus calcarea in a continuous pattern[12]. No pores were visible on *C. hattini*, *H. verticalis*, or *Squalicorax* spp.[12]. Very small pores are scattered across the lateral faces of *C. carcharias* and *C. maximus*[12]. No fine radial canals are present on the inner surface of the corpus calcareum similar to *C. ricki*[12].

Bands and growth characteristics

The birth ring may be associated with an angle change on the exterior surface of the corpus calcareum in NTM P922-29 and NTM P922-33. The birth ring is marked by a concentric ridge and followed by a dark post birth ring. The presence of a prebirth ring suggests the embryo deposited an annulus before birth. Bands are terminated with a broad dark ring and a concentric ridge on the surface of the corpus calcareum. Annuli are recognized by a concentric ridge, broad dark ring that extends between the corpora calcarea across the radial lamella. These dark, annular rings are interspersed with lighter, broad rings to form the complete band.

Macrophagy

There are no teeth associated with the Darwin Formation cardabiodontid. However, the centra possesses many morphological hallmarks of a macrophagous shark. For example, the corpora calcarea possess well-defined annuli that are uniformly thick. In addition, the centra are shortened to increase flexibility of the vertebral column, unlike the gigantic microphagous lamniform *C. maximus*. There are only thin concentric lamellae in the Darwin Formation cardabiodontid. *C. maximus* otherwise possesses greatly thickened concentric lamellae. The radial lamellae are relatively thin and gracile in the Darwin Formation cardabiodontid, unlike those of *Rhincodon typus*, which possesses layered, broad lamellae.

Size estimation

Data collection and pre-processing

The extraction of measurement data from static images was achieved using image digitization via the WebPlotDigitizer online tool (https://automeris.io/). Procedurally, images were imported one at a time and the axes (x and y) calibrated using the original scales as a reference and lastly followed by point digitization of labelled points (labelling was done in CorelDraw v. 24.5.0.731 as a pre-processing step to allow for controlled and repeatable digitization). Measurement error (digitization error) was assessed by digitizing the labelled points in each graph five times. We used the *irr* v. 0.84.1 R package to compute the intraclass correlation coefficient (ICC) for one-way models. ICC values equal to or greater than 0.9 was interpreted as excellent agreement between digitized datasets (Supplementary Table 3). For scrapped data we generated average species datasets (based on the five replicates) that was subsequently used for the main analysis.

Scaling equations

We provide a summary of each species included in our extant dataset along with information relevant to our data treatment and analysis.

*Alopias pelagicu*s. Data were extracted from Liu *et al.*[25] that shows the relationship between centrum radius (mm) and precaudal length (cm) in 269 individual *A. pelagicus* (155 females and 114 males) caught in Taiwanese waters. In total, we managed to digitize 173 points from the original point scatter. The following scaling equation was used to convert to total length (TL):

$$TL_{female} = 2.34 + 1.93 \times PCL$$

We supplemented these records with raw data (N=157) provided by Drew *et al.*[26].

Alopias superciliosus. Data were extracted from Liu *et al.*[27] that shows the relationship between centrum radius (mm) and precaudal length (cm) in 321 individual *A. superciliosus*. Despite, the low image-resolution and extensive overplotting, we managed to digitize 226 data points (70.4%) (155 female and 71 male). The following equations were provided by Liu *et al.*[27] for converting male and female individual *A. superciliosus* to total length:

$$TL_{female} = 15.3 + 1.81 \times PCL$$

$$TL_{male} = 15.1 + 1.76 \times PCL$$

Alopias vulpinus. Data were extracted from Cailliet *et al*.[28] that shows the relationship between centrum diameter (mm) and total length (mm) in 67 individual *A. vulpinus*. We managed to digitize all points. No body length conversion was required.

Carcharias taurus. Data were extracted from Lucifora[29] that shows the relationship between centrum radius (mm) and total length (cm) of 85 individual *C. taurus*. We managed to digitize 76 points.

Carcharodon carcharias. Raw morphometric data of 114 individuals from the coast of South Africa were derived from Wintner & Cliff[30].The data includes information on sex, body mass, precaudal length, and centrum diameter. The body mass of 3 individuals was missing so we omitted these observations to create a matching dataset with both precaudal length and mass availability (N = 111). Precaudal length was subsequently converted using the following equation:

$$TL = 1.251\ PCL + 5.207$$

We supplemented these records with data scrapped from Cailliet *et al*.[31] that includes 18 individuals captured in California waters and measured as centrum diameter (mm) and total length (mm).

Cetorhinus maximus. Data were extracted from Natanson *et al*.[24] that show the relationship between dorsal centum diameter (cm) and total length (cm) of 21 individual *C. maximus*. Points indicated by a tringle symbol in the original main text figure represent centrum diameter and were all digitized.

Isurus oxyrinchus. Our main source of *I. oxyrinchus* measurements relied on the raw data from Natanson *et al*.[32]. The data includes vertebral radius (mm) and fork length (cm) measurements for 236 non-embryonic individuals (108 males and 128 females) from the North Atlantic Ocean. The following equation was provided in Natanson *et al*.[32]:

$$FL = 0.9286\ (TL) - 1.7101$$

We rearranged the equation to obtain TL as such:

$$TL = (FL + 1.7101)/0.9286$$

Lamna ditropis. Data were extracted from Goldman & Musick[33] that show the relationship between centrum radius (mm) and precaudal length (cm) of individuals captured in the eastern North Pacific (N=182). We managed to digitize 143 points (78.57%). Conversion to total length was achieved using the following equation:

$$TL = (1.15\ \times PCL) + 15.19$$

Lamna nasus. Our main source of *L. nasus* measurements relied on the raw data from Natanson *et al*.[34]. The data includes vertebral radius (mm) and fork length (cm) measurements of 575 non-embryonic individuals (283 males and 292 females) from the Western North Atlantic Ocean. The following equation was used to convert to total length:

$$FL = 0.885\ (TL) + 0.99$$

And rearranged:

$$TL = (FL + 0.99)/0.885$$

Pseudocarcharias kamoharai. Data was extracted from Kindong *et al*.[35] that shows the relationship between vertebral radius (mm) and fork length (cm) in 114 individual *P. kamoharai* captured in the Eastern Atlantic Ocean. We managed to digitize 110 points (96.49%) from the original graph. The following equation was provided in the main text:

$$FL = (TL + 0.3496)/1.1513$$

We rearranged the equation to find the value for TL:

$$TL = (FL \times 1.1513) - 0.3496$$

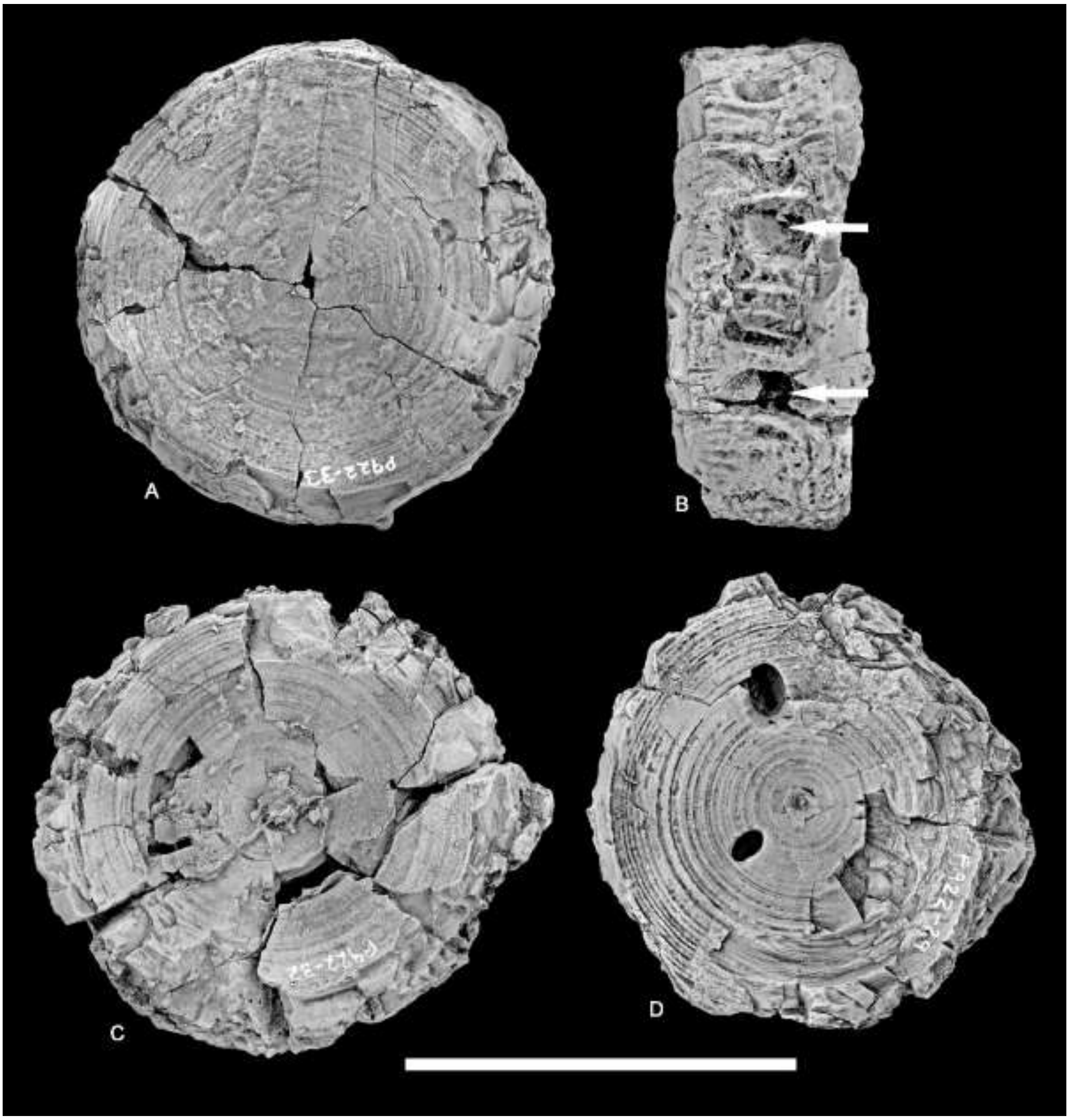

Supplementary Fig. 1. Darwin Formation cardabiodontid precaudal vertebral centra. NTM P922-33 in **(A)** anterior or posterior, and **(B)** dorsal(?) views showing pits for the neural arch or transverse processes (arrows). **(C)** NTM P922-32 in anterior or posterior view. **(D)** NTM P922-29 in anterior or posterior view. Scale bar = 100 mm.

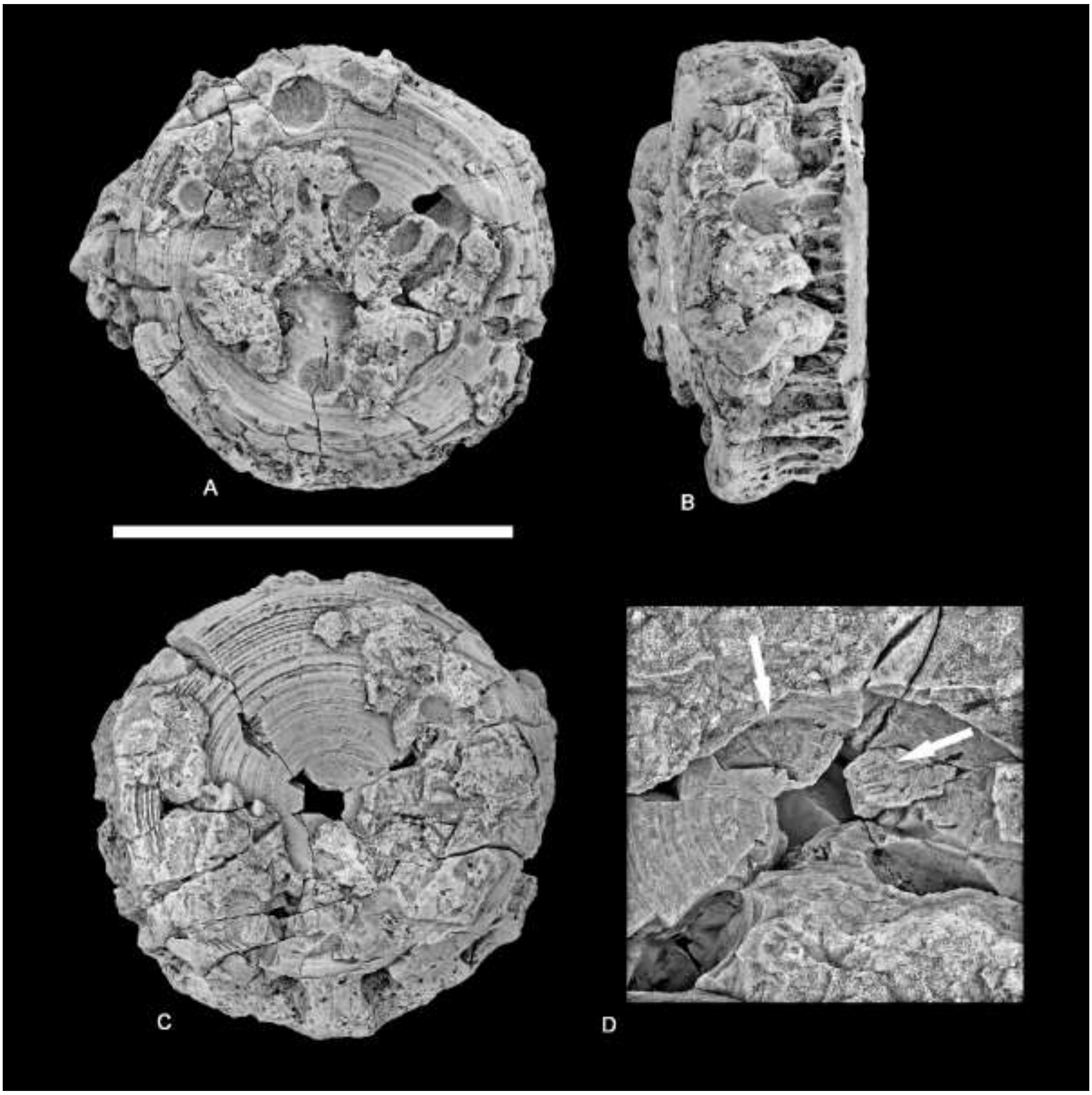

Supplementary Fig. 2. Darwin Formation cardabiodontid precaudal vertebral centra. NTM P922-37 in **(A)**, anterior or posterior, and **(B)**, lateral views. NTM P9382 in **(C)** anterior or posterior view with **(D)** enlargement (opposing articular surface) showing the radial lamellae (arrows). Scale bar in **(A-C)** = 100 mm.

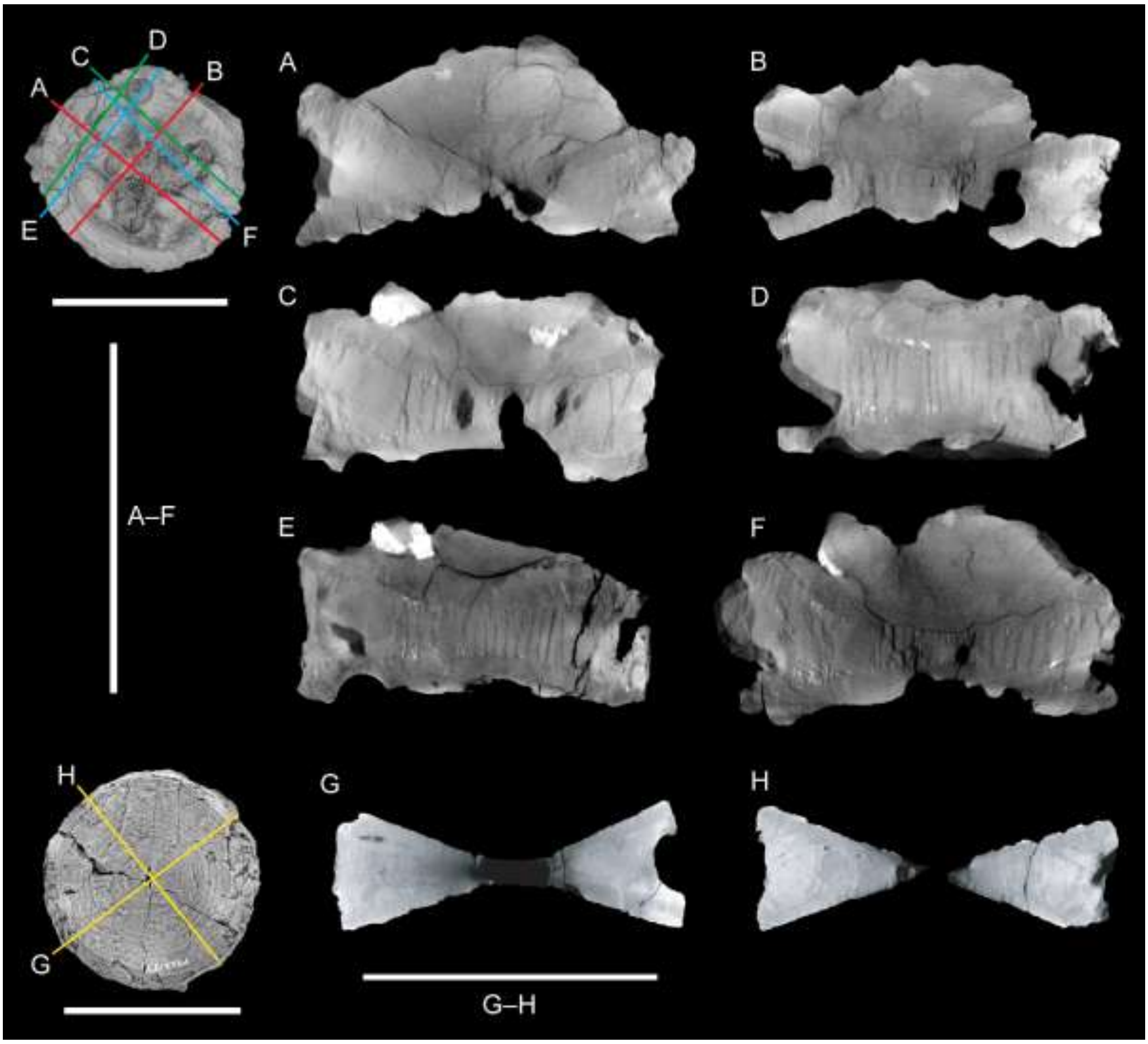

Supplementary Fig. 3. Scan sections of the Darwin Formation cardabiodontid precaudal vertebral centra. (A-F) NTM P922-37; **(G-H)** NTM P922-33. Scale bars = 100 mm.

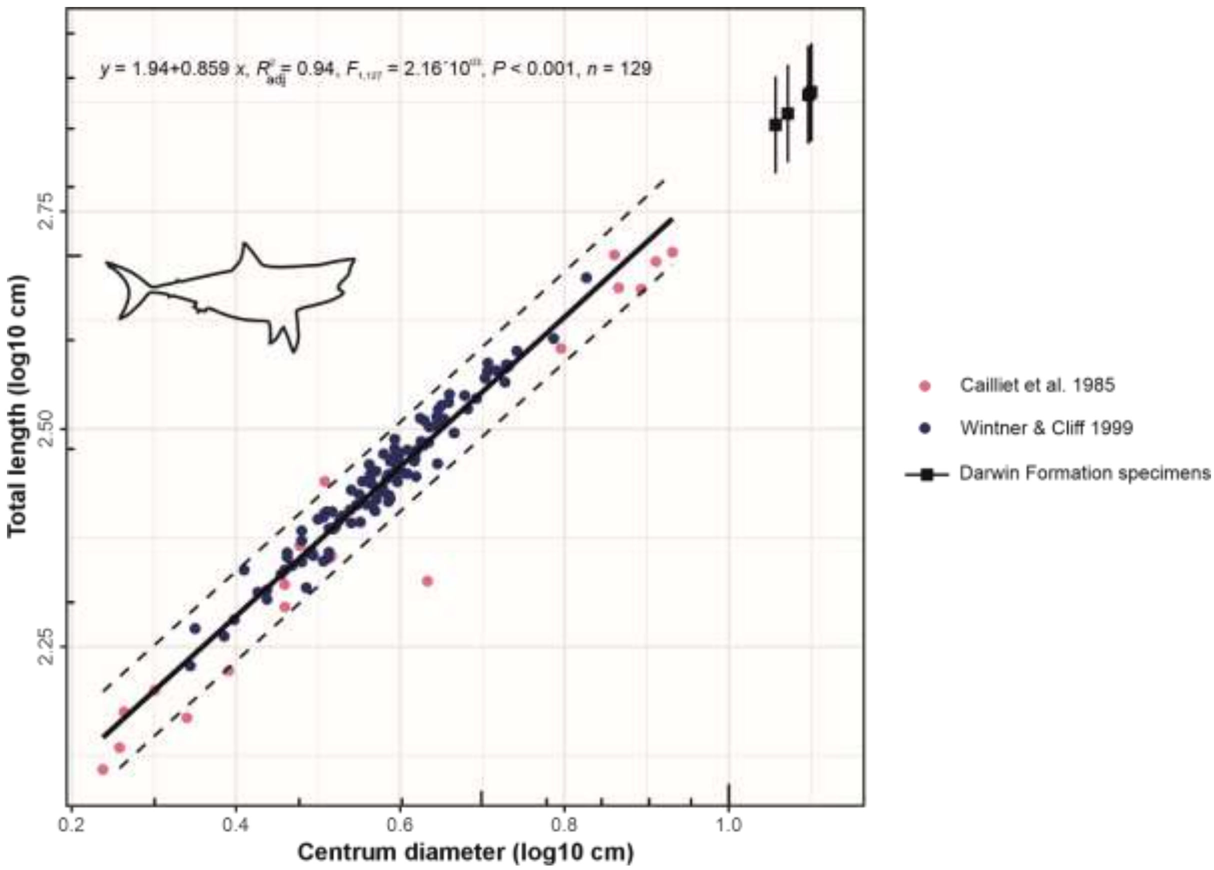

Supplementary Fig. 4. Relationship between CD and TL in *Carcharodon carcharias*. Data from Wintner & Cliff[30] and Cailliet *et al*.[31]. The estimated TL with 95% prediction intervals for the Darwin Formation cardabiodontid specimens are also shown in the graph. Graphic silhouette reproduced with permission from Gray Taxidermy (Pompano Beach, U.S.A.). Abbreviations explained in the main text.

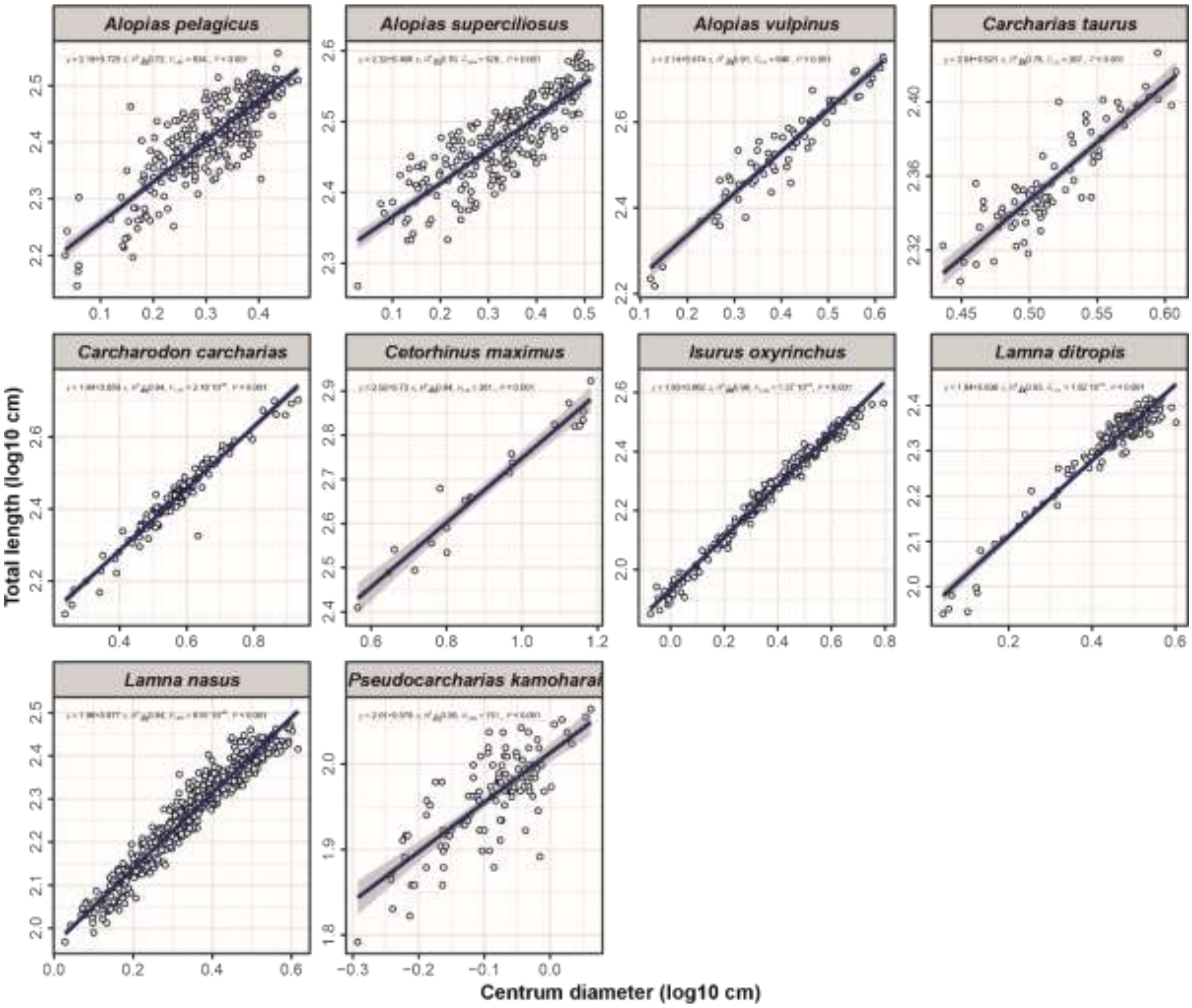

Supplementary Fig. 5. Linear regression of log10-transformed CD and TL in lamniform species. Shaded 95% confidence interval represent the uncertainty around the mean predicted relationship. Abbreviations explained in the main text.

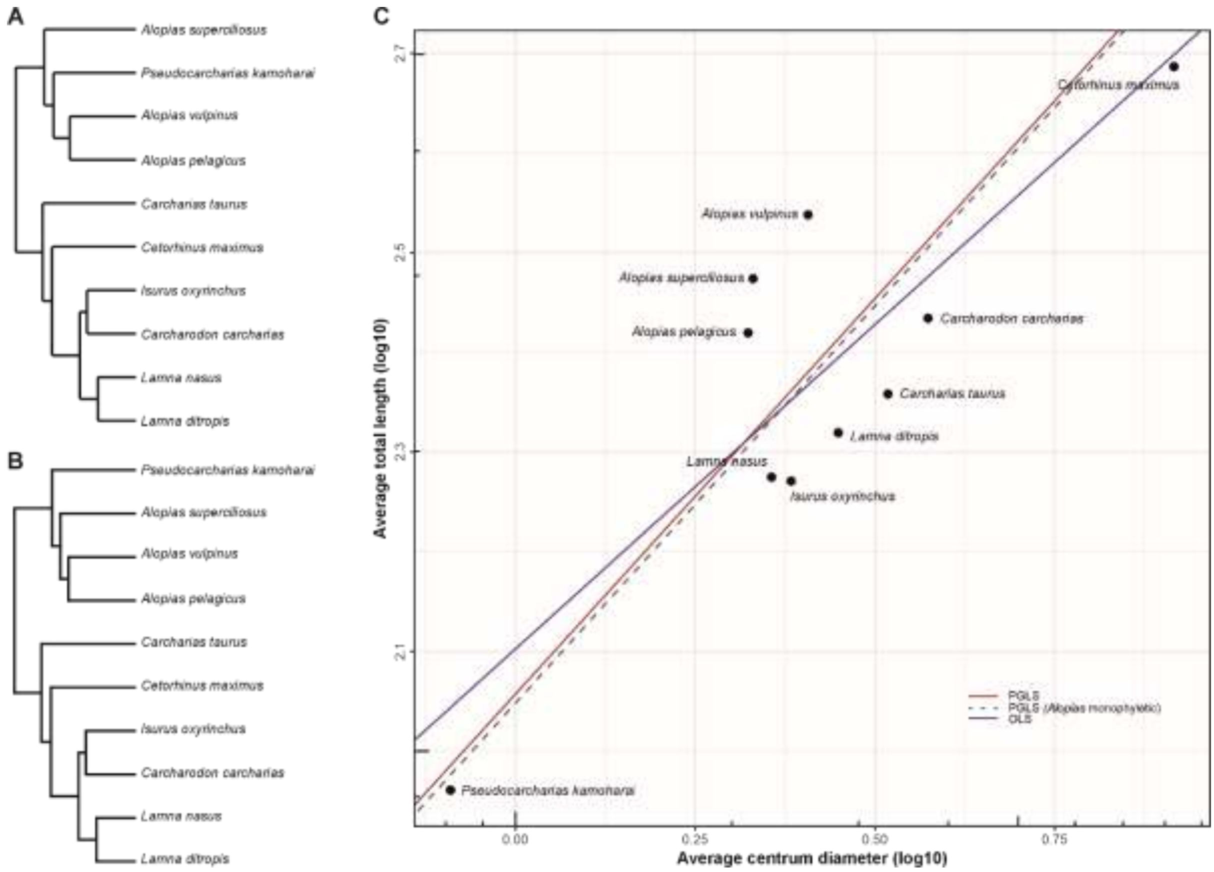

Supplementary Fig. 6. OLS versus PGLS model fits. Maximum clade credibility tree of lamniform shark species **(A)** and **(B)** an alternate topology showing *Alopias* as monophyletic. **(C)** Bivariate plot showing the relationship between the logarithms of average CD and TL with lines of best fit from both OLS and PGLS model fits. Abbreviations explained in the main text.

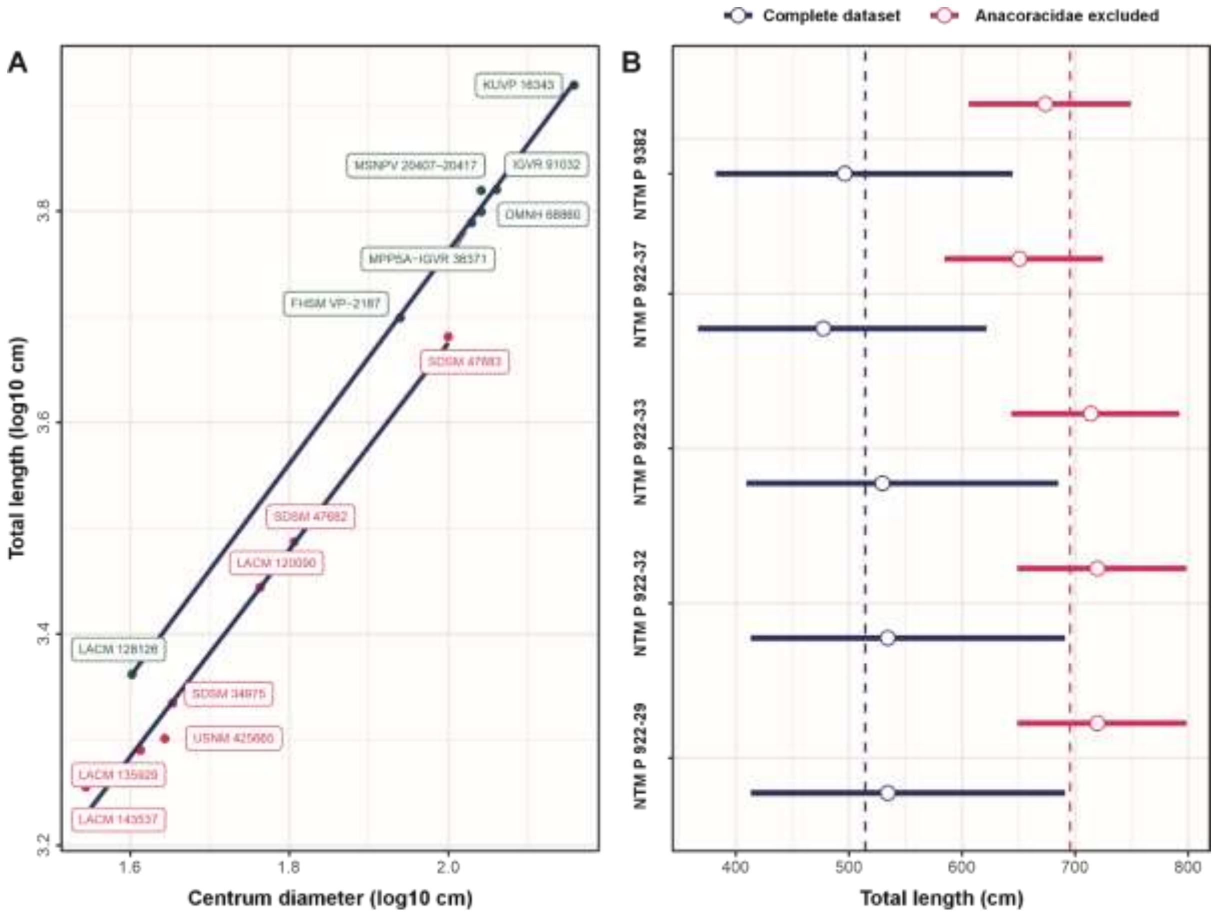

Supplementary Fig. 7. Linear model fit and TL estimates from using a Cretaceous taxon dataset. (A) Relationship between the log-CD and log-TL in Anacoracidae and non-Anacoracidae species. **(B)** Predicted TL in the Darwin Formation cardabiodontid vertebral centra along with 95% prediction intervals computed from the complete dataset (N=15) and a reduced sample that includes Anacoracidae species only. Dotted lines represent the average fitted values. Abbreviations explained in the main text.

Supplementary Table 1. Summary statistics and data sources for the extant taxon sample. Sample size (N = 1912), size range (TL of each species sample), data sources, and source references are provided. Abbreviations explained in the main text.

Species	N	Size range (cm)	Source Type	Reference
Alopias pelagicus	329	140-361	Data Scraped & Original Paper	[25,26]
Alopias superciliosus	226	185-396	Data Scraped	[27]
Alopias vulpinus	67	165-565	Data Scraped	[13]
Carcharias taurus	76	201-267	Data Scraped	[29]
Carcharodon carcharias	129	129-505	Data Scraped & Original Paper	[30,31]
Cetorhinus maximus	21	257-837	Data Scraped	[24]
Isurus oxyrinchus	236	71-366	Original Paper	[32]
Lamna ditropis	143	87-260	Data Scraped	[33]
Lamna nasus	575	93-295	Original Paper	[34]
Pseudocarcharias kamoharai	110	62-116	Data Scraped	[35]

Supplementary Table 2. Fossil taxon sampling. CD and TL measurement (cm) data compiled for 15 Cretaceous lamniform taxa. Abbreviations explained in the main text.

Species	Specimen	CD	TL	Age	Reference
Cretodus sp.	IGVR 91032	11.5	661	middle Turonian	[36]
Cretoxyrhina mantelli	FHSM VP-2187	8.7	500	late Coniacian–middle Santonian	[37]
Cretalamna hattini	LACM 128126	4	230	late Santonian-early Campanian	[38]
Lamniform sp.	OMNH 68860	11	630	Albian	[17]
Cretoxyrhina mantelli	MPPSA-IGVR 36371	10.7	615	Turonian-Coniacian	[39]
Cretoxyrhina mantelli	MSNPV 20407–20417	11	660	early Santonian	[40]
Lamniformes sp.	KUVP 16343	14.4	830	late Albian	[18]
Squalicorax hartwellii	USNM 425665	4.4	200	late Coniacian-early Campanian	[41]
Squalicorax hartwellii	LACM 135929	4.1	195	late Coniacian-early Campanian	[41]
Squalicorax hartwellii	LACM 143537	3.5	180	late Coniacian-early Campanian	[41]
Squalicorax hartwellii	LACM 120090	5.8	278	late Coniacian-early Campanian	[41]
Squalicorax crassidens	SDSM 34975	4.5	216	middle Campanian	[41]
Squalicorax crassidens	SDSM 47682	6.4	307	middle Campanian	[41]
Squalicorax crassidens	SDSM 47683	10.0	480	middle Campanian	[41]
Cardabiodon ricki	WAM 96.4.45.108	8.95	-	Cenomanian	[42]

Supplementary Table 3. Interrater reliability measured as intraclass correlation coefficient (ICC) for one-way models. Subjects = the number of subjects examined; Value = the intraclass correlation coefficient.

Subjects	Raters	Value	Variable	Species	Interpretation
173	5	0	CD	*Alopias pelagicus*	Excellent agreement
173	5	0	TL	*Alopias pelagicus*	Excellent agreement
226	5	0	CD	*Alopias superciliosus*	Excellent agreement
226	5	0	TL	*Alopias superciliosus*	Excellent agreement
67	5	0	CD	*Alopias vulpinus*	Excellent agreement
67	5	0	TL	*Alopias vulpinus*	Excellent agreement
76	5	0	CD	*Carcharias taurus*	Excellent agreement
76	5	0	TL	*Carcharias taurus*	Excellent agreement
18	5	0	CD	*Carcharodon carcharias*	Excellent agreement
18	5	0	TL	*Carcharodon carcharias*	Excellent agreement
21	5	0	CD	*Cetorhinus maximus*	Excellent agreement
21	5	0	TL	*Cetorhinus maximus*	Excellent agreement
143	5	0	CD	*Lamna ditropis*	Excellent agreement
143	5	0	TL	*Lamna ditropis*	Excellent agreement
110	5	0	CD	*Pseudocarcharias kamoharai*	Excellent agreement
110	5	0	TL	*Pseudocarcharias kamoharai*	Excellent agreement

Supplementary references

1. Turner, S. & Rozefelds, A. Tip of the pyramid? Cretaceous megasharks from Australia. *The Beagle: Records of the Northern Territory Museum of Arts and Sciences* **9**, 262–263 (1992).

2. Kear, B. P. & Hamilton-Bruce, R. J. *Dinosaurs in Australia. Mesozoic Life from the Southern Continent*. (CSIRO Publishing, 2011).

3. Henderson, R. A. Eustatic and palaeoenvironmental assessment of the mid-Cretaceous Bathurst Island Group of the Money Shoals Platform, northern Australia. *Palaeogeogr Palaeoclimatol Palaeoecol* **138**, 115–138 (1998).

4. Smart, J. & Senior, B. R. Jurassic— Cretaceous basins of northeastern Australia. in *The Geology and Geophysics of Northeastern Australia* (eds. Henderson, R. A. & Stephenson, P. J.) 315–318 (Geological Society of Australia, Queensland Division, Brisbane, 1980).

5. Williamson, T. Systematics and biostratigraphy of Australian Early Cretaceous belemnites with contributions to the timescale and palaeoenvironmental assessment of the Australian Early Cretaceous system derived from stable isotope proxies. (James Cook University, Townsville, Queensland, Australia, 2006).

6. Jell, P. A. & Cook, A. G. An annotated checklist of Australian Mesozoic marine macroinvertebrates. *Alcheringa: An Australasian Journal of Palaeontology* **49**, 114–497 (2025).

7. Partridge, A. D. Jurassic – Early Cretaceous spore-pollen and dinocyst zonations for Australia. in *Australian Mesozoic and Cenozoic Palynology Zonations – updated to the 2004 Geologic Time Scale* (Geoscience Australia Record 2006/23, 2006).

8. Kear, B. P. Darwin Formation (Early Cretaceous, Northern Territory) marine reptile remains in the South Australian Museum. *Records of the South Australian Museum* **35**, 33–47 (2002).

9. Kear, B. P. Cretaceous marine reptiles of Australia: a review of taxonomy and distribution. *Cretac Res* **24**, 277–303 (2003).

10. Kear, B. P., Fordyce, R. E., Hiller, N. & Siversson, M. A palaeobiogeographical synthesis of Australasian Mesozoic marine tetrapods. *Alcheringa: An Australasian Journal of Palaeontology* **42**, 461–486 (2018).

11. Kozuch, L. & Fitzgerald, C. A guide to identifying shark centra from southeastern archaeological sites. *Southeastern Archaeology* 146–157 (1989).

12. Newbrey, M., Siversson, M., Cook, T. D., Fotheringham, A. M. & Sanchez, R. L. Vertebral morphology, dentition, age, growth, and ecology of the large lamniform shark Cardabiodon ricki. *Acta Palaeontol Pol* **60**, 877–897 (2015).

13. Cailliet, G. M., Martin, L. K., Kusher, D., Wolf, P. & Welden, B. A. Techniques for enhancing vertebral bands in age estimation of California elasmobranchs. in *Proceedings of the International Workshop on Age Determination of*

Oceanic Pelagic Fishes: Tunas, Billfishes, and Sharks (eds. Prince, E. D. & Pulos, L. M.) vol. 8 157–165 (National Oceanic and Atmospheric Administration Technical Report, National Marine Fisheries Service, 1983).

14. Cailliet, G. M., Smith, W. D., Mollet, H. F. & Goldman, K. J. Age and growth studies of chondrichthyan fishes: the need for consistency in terminology, verification, validation, and growth function fitting. *Environ Biol Fishes* **77**, 211–228 (2006).

15. Cailliet, G. M. & Goldman, K. J. Age determination and validation in chondrichthyan fishes. in *The Biology of Sharks and their Relatives* (eds. Carrier, J., Musick, J. A. & Heithaus, J. M.) 399–447 (CRC Press, Boca Raton, 2004).

16. Ridewood, W. G. & MacBride, E. W. VIII.—On the calcification of the vertebral centra in sharks and rays. *Philosophical Transactions of the Royal Society of London. Series B, Containing Papers of a Biological Character* **210**, 311–407 (1921).

17. Frederickson, J. A., Schaefer, S. N. & Doucette-Frederickson, J. A. A Gigantic Shark from the Lower Cretaceous Duck Creek Formation of Texas. *PLoS One* **10**, e0127162 (2015).

18. Shimada, K. Gigantic lamnoid shark vertebra from the Lower Cretaceous Kiowa Shale of Kansas. *J Paleontol* **71**, 522–524 (1997).

19. Kriwet, J., Mewis, H. & Oliver, H. A partial skeleton of a new mackerel shark (Chondrichthyes, Lamniformes) from the Miocene of Europe. *Acta Palaeontol Pol* **60**, 857–875 (2014).

20. Cook, T. D. *et al.* A partial skeleton of the Late Cretaceous lamniform shark, *Archaeolamna kopingensis* , from the Pierre Shale of western Kansas, U.S.A. *J Vertebr Paleontol* **31**, 8–21 (2011).

21. Siversson, M., Lindgren, J., Newbrey, M. G., Cederström, P. & Cook, T. D. Late Cretaceous (Cenomanian-Campanian) mid-palaeolatitude sharks of Cretalamna appendiculata type. *Acta Palaeontol Pol* **60**, 339–384 (2015).

22. Moore, G. I. & Newbrey, M. G. Whale shark on a white shark's menu. *Marine Biodiversity* **46**, 745–746 (2016).

23. Shimada, K. Ontogenetic parameters and life history strategies of the late Cretaceous lamniform shark, Cretoxyrhina mantelli, based on vertebral growth increments. *J Vertebr Paleontol* **28**, 21–33 (2008).

24. Natanson, L. *et al.* Ontogenetic vertebral growth patterns in the basking shark Cetorhinus maximus. *Mar Ecol Prog Ser* **361**, 267–278 (2008).

25. Liu, K. M., Chen, C. T., Liao, T. H. & Joung, S. J. Age, Growth, and Reproduction of the Pelagic Thresher Shark, Alopias Pelagicus in the Northwestern Pacific. *Copeia* 68–74 (1999).

26. Drew, M., White, W. T., Dharmadi, Harry, A. V. & Huveneers, C. Age, growth and maturity of the pelagic thresher *Alopias pelagicus* and the scalloped hammerhead *Sphyrna lewini*. *J Fish Biol* **86**, 333–354 (2015).

27. Liu, K. M., Chiang, P. J. & Chen, C. T. Age and Growth Estimates of the Bigeye Thresher Shark, Alopias Superciliosus, in Northeastern Taiwan Waters. *Fishery Bulletin* **96**, 482–491 (1998).

28. Cailliet, G. M., Martin, L. K., Harvey, J. T., Kusher, D. & Welden, B. A. Preliminary studies on the age and growth of blue (Prionace glauca), common thresher (Alopias vulpinus), and shortfin mako (Isurus oxyrinchus) sharks from California waters. in *Proceedings International Workshop on Age Determination of Oceanic Pelagic Fishes: Tunas, Billfishes, Sharks* 179–188 (NOAA Tech. Rep. NMFS, 1983).

29. Lucifora, L. O. Ecología y conservación de los grandes tiburones costeros de Bahía Anegada. (Universidad Nacional de Mar del Plata, Buenos Aires, 2003).

30. Wintner, S. P. & Cliff, G. Age and growth determination of the white shark, Carcharodon carcharias, from the east coast of South Africa. *Fishery Bulletin, U. S* **97**, 153–169 (1999).

31. Cailliet, G. M., Natanson, L. J., Welden, B. A. & Ebert, D. A. Preliminary studies on the age and growth of the white shark, Carcharodon carcharias, using vertebral bands. *Memoirs of the Southern California Academy of Sciences* **4**, 49–60 (1985).

32. Natanson, L. J. *et al.* Validated age and growth estimates for the shortfin mako, Isurus oxyrinchus, in the North Atlantic Ocean. *Environ Biol Fishes* **77**, 367–383 (2006).

33. Goldman, K. J. & Musick, J. A. Growth and Maturity of Salmon Sharks (Lamna Ditropis) in the Eastern and Western North Pacific, and Comments on Back-Calculation Methods. *Fishery Bulletin* **104**, 278–292 (2006).

34. Natanson, L. J., Mello, J. J. & Campana, S. E. Validated Age and Growth of the Porbeagle Shark (Lamna Nasus) in the Western North Atlantic Ocean. *Fishery Bulletin* **100**, 266–278 (2002).

35. Kindong, R., Wang, H., Wu, F., Dai, X. & Tian, S. Age, Growth, and Sexual Maturity of the Crocodile Shark, Pseudocarcharias kamoharai, From the Eastern Atlantic Ocean. *Front Mar Sci* **7**, (2020).

36. Amalfitano, J. *et al.* Direct evidence of trophic interaction between a large lamniform shark, Cretodus sp., and a marine turtle from the Cretaceous of northeastern Italy. *Palaeogeogr Palaeoclimatol Palaeoecol* **469**, 104–121 (2017).

37. Shimada, K. Skeletal anatomy of the late cretaceous lamniform shark, cretoxyrhina mantelli from the Niobrara Chalk in Kansas. *J Vertebr Paleontol* **17**, 642–652 (1997).

38. Shimada, K. Skeletal and dental anatomy of lamniform shark, Cretalamna appendiculata, from Upper Cretaceous Niobrara Chalk of Kansas. *J Vertebr Paleontol* **27**, 584–602 (2007).

39. Amalfitano, J. *et al.* Large deadfalls of the 'ginsu' shark Cretoxyrhina mantelli (Agassiz, 1835) (Neoselachii, Lamniformes) from the Upper Cretaceous of northeastern Italy. *Cretac Res* **98**, 250–275 (2019).

40. Larocca Conte, G. *et al.* Reassessment of a large lamniform shark from the Upper Cretaceous (Santonian) of Italy. *Cretac Res* **99**, 156–168 (2019).

41. Shimada, K. & Cicimurri, D. J. Skeletal anatomy of the Late Cretaceous shark,Squalicorax (Neoselachii: Anacoracidae). *Palaontol Z* **79**, 241–261 (2005).

42. Siverson, M. A new large lamniform shark from the uppermost Gearle Siltstone (Cenomanian, Late Cretaceous) of Western Australia. *Trans R Soc Edinb Earth Sci* **90**, 49–66 (1999).